Optimization of lamp arrangement in a closed-conduit UV reactor based on a genetic algorithm

Tipu Sultan, Zeshan Ahmad and Jinsoo Cho

ABSTRACT

The choice for the arrangement of the UV lamps in a closed-conduit ultraviolet (CCUV) reactor significantly affects the performance. However, a systematic methodology for the optimal lamp arrangement within the chamber of the CCUV reactor is not well established in the literature. In this research work, we propose a viable systematic methodology for the lamp arrangement based on a genetic algorithm (GA). In addition, we analyze the impacts of the diameter, angle, and symmetry of the lamp arrangement on the reduction equivalent dose (RED). The results are compared based on the simulated RED values and evaluated using the computational fluid dynamics simulations software ANSYS FLUENT. The fluence rate was calculated using commercial software UVCalc3D, and the GA-based lamp arrangement optimization was achieved using MATLAB. The simulation results provide detailed information about the GA-based methodology for the lamp arrangement, the pathogen transport, and the simulated RED values. A significant increase in the RED values was achieved by using the GA-based lamp arrangement methodology. This increase in RED value was highest for the asymmetric lamp arrangement within the chamber of the CCUV reactor. These results demonstrate that the proposed GA-based methodology for symmetric and asymmetric lamp arrangement provides a viable technical solution to the design and optimization of the CCUV reactor.

Key words | fluence rate, genetic algorithms, RED, UV reactor, UV lamps, water disinfection

Tipu Sultan (corresponding author)
Jinsoo Cho
Department of Mechanical Engineering,
Hanyang University,
Haengdang-dong, Sungdong-gu,
Seoul 133-791,
Republic of Korea
E-mail: *sultan.sindhu@gmail.com*

Zeshan Ahmad
Department of Mechanical Engineering,
School of Engineering (SEN),
University of Management & Technology,
Lahore,
Pakistan

NOMENCLATURE

A and B	constants in the logarithm microbial inactivation rate function	[–]
D_c	CCUV reactor chamber diameter	[m]
dt	pathogens residing time	[s]
F_D	drag force	[N]
I	intensity of UV radiation	[W/m^2]
K	inactivation rate constant	[m^2/mJ]
K_{inlet}	turbulent kinetic energy	[m^2/s^2]
N	pathogen influent	[–]
N_0	pathogens effluent	[–]
N/N$_0$	log inactivation	[–]
P	lamp power	[W]
R_{12}, R_{23}	reflectivities of the media	[–]
T_q, T_w	transmissivities of quartz and water	[–]
t	time	[s]
u_{inlet}	velocity at inlet	[m/s^2]
ε_{inlet}	turbulent dissipation at inlet	[m^2/s^3]
ρ	density	[kg/m^3]

Subscripts

i, j position of a cell
inlet inlet

INTRODUCTION

A water-disinfection UV reactor consists of a reaction vessel that contains a number of UV lamps. The UV lamps are protected from the water by the quartz sleeves surrounding them. The water enters the reactor and flows around the quartz sleeves. The pathogens present in the water travel through the reactor and are irradiated by the UV light. Microbial transport is simulated using the Lagrangian particle tracking method (Munoz *et al.* 2007). UV intensity (fluence rate) depends on the relative positions of the

doi: 10.2166/wst.2016.119

particle and the UV lamps. The UV dose received by the pathogens depends on two factors: the trajectories through the reactor and the fluence rate.

The fluence rate is dependent on the positions of the UV lamps within the UV reactor. The lamp arrangement simultaneously affects the fluence rate distribution and the flow of the water within the UV reactor. Two lamp arrangements are commonly used: parallel to the reactor axis and perpendicular to the reactor axis. The parallel arrangement results in greater fluence rate, but the UV fluence rate is much lower at the two reactor ends and near the reactor outer wall. The perpendicular arrangement provides a more uniform UV fluence rate distribution within the radiation zone, but there is almost no UV radiation outside the radiation zone. Taghipour (2004) examined six lamp arrangements in the UV reactor and found the performance is greatly dependent on the arrangement. In addition, Taghipour & Sozzi (2005) compared the degradation of the organic material for two lamp arrangements and concluded the degradation to be dependent on the lamp arrangement within the cross-flow UV reactor. A major drawback seen in the studies (Taghipour 2004; Taghipour & Sozzi 2005) is the unavailability of a viable systematic methodology for determining the lamp arrangement.

Ray (1999) classified the UV light sources into three types: external, distributive, and immersive. Because the immersive reactors have more output and are more common in industrial applications, we analyzed immersive reactors in this study. Xu *et al.* (2013) found that the relationship between the UV reactor performance and its operating variables is complicated and cannot be modelled by simple correlation. Moreover, Xu *et al.* (2015) conducted a performance analysis of lamp arrangement for an annular reactor on common basis. They found that different lamp arrangements have different fluence rate distributions and water flow profiles inside the reactors, affecting the reactor performance complexly.

Genetic algorithms (GAs) are a metaheuristic approach to generate useful solutions for complex problems (Renner & Ekárt 2003). There are two predominant reasons for the use of GAs for lamp arrangement optimization. First, the objective function generally has multiple local extrema, whereas the aim is to search for the global extremum. These types of problems cannot be solved using classical approaches (e.g. gradient methods) because they only evaluate the local extrema. In such complex problems, GAs may offer solutions to the problems (Renner & Ekárt 2003). Second, the objective function is discontinuous, nondifferentiable, stochastic, or highly nonlinear. Therefore, the use of GA methodology was requisite in the present study. Xu *et al.* (2014) performed modeling and optimization of the UV reactor by using a GA-based model and an artificial neural network (ANN)–based model. They validated the results using computational fluid dynamics (CFD) and found the GA-based model to be better at prediction than the ANN-based model. They were more focused on the input variables and size of the UV reactor. Whereas the current research is more focused on lamp positioning optimization using GP.

To date, a viable systematic methodology for the arrangement of the lamps within the chamber of a cross-flow closed-conduit UV (CCUV) reactor is not well defined in the literature and is at its initial stage of research. A viable systematic methodology based on a GA is proposed for lamp arrangement optimization in this research work. The objective function is the reduction equivalent dose (RED), and the goal is to achieve the optimum lamp arrangement for maximum RED of the CCUV reactor. Both symmetric and asymmetric lamp arrangements were considered for the performance optimization in this research work.

MATHEMATICAL MODELING OF A WATER-DISINFECTION CCUV REACTOR

A schematic diagram illustrating the sub-processes of the CCUV reactor is shown in Figure 1. UV water disinfection can be represented by a combination of four sub-models: a flow model, a fluence rate model, a kinetic model, and a discrete phase model (DPM). To improve water disinfection, a detailed understanding of all these sub-models is important.

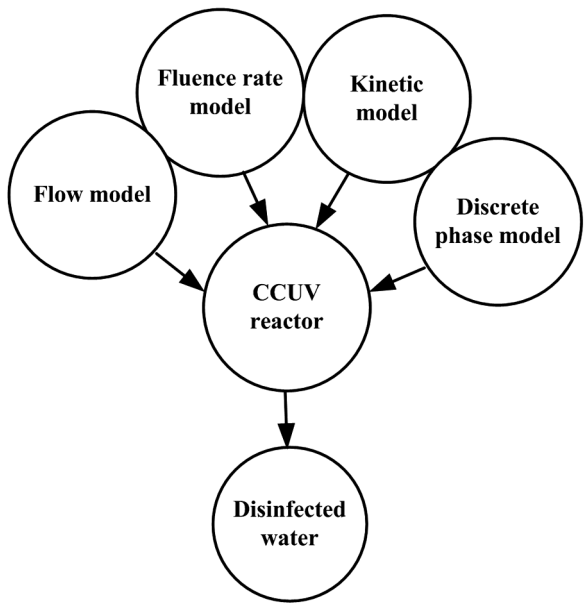

Figure 1 | Schematic of a water-disinfection CCUV reactor.

Flow model

The flow through the reactor was modelled for turbulent settings on the basis of Reynolds number of 2.72×10^5. The standard two-equation k-ε turbulent flow model is employed to simulate the fluid flow field through the UV reactor. This is a well-established two-equation model successfully employed for many engineering applications (Launder & Spalding 1974). It utilizes the Reynolds-averaged Navier–Stokes (RANS) governing equations for conservation of mass and conservation of momentum in conjunction with a turbulence model at discrete locations within the physical domain.

Discrete phase model

The motion of a pathogen in the UV reactor is tracked by the DPM. The DPM equation is a combination of three forces: drag force, gravity force, and additional forces, such as in Equation (1):

$$du_p/dt = \underbrace{F_D(u-u_p)}_{\text{Drag force}} + \overbrace{g_x(\rho_p-\rho/\rho_p)}^{\text{Gravity force}} + \underbrace{F_x}_{\text{Additional force}} \quad (1)$$

Here, u and ρ are the water phase velocity and density, u_p and ρ_p are the pathogen velocity and density, F_D is the drag force, and F_x represents additional forces including pressure gradient, thermophoresis, rotating reference frame, Brownian motion, Saffman lift, and others (user defined). Further details about DPM and these parameters can be found elsewhere (Fluent 2012).

The pathogens were injected at the inlet by defining an injection. The injection provides the information about the types of pathogens (inert, droplet, or combusting particle), the material of the pathogens, and the initial conditions. The initial conditions include the mass flow rate of the injected pathogens, the diameter of the pathogens, the number of injected pathogens, and the desired plane for the injection of the pathogens. The parameters used for the pathogens' injection in the DPM model are obtained from the literature (Munoz *et al.* 2007) and listed in Table 1.

The individual pathogen trajectory is calculated by using the Lagrangian reference frame. The mass and the surface area of each pathogen are given at each step. Therefore, the solver can calculate the force balance applied to the pathogen at each pathogen step. The overall pathogen trajectory can be determined by adding the paths of all these individual steps.

Table 1 | Pathogens properties

Parameters	Details
Pathogens inlet boundary condition	Fully developed turbulent flow velocity profile
Pathogens outlet boundary condition	Escape
Number of injected pathogens	3,000
Lagrangian empirical constant	0.15
Length scale	$2.0 \times 10^{-4} m$
Pathogens properties	$\rho = 1000\ Kg/m^3,\ T = 293.15\ K$
Pathogens diameter	$1.0 \times 10^{-4} m$
DPM	DRW
Maximum number of steps	5.0×10^4

To obtain more realistic physical results, the effect of turbulence dispersion on the pathogen was modeled using stochastic tracking. In ANSYS FLUENT, the stochastic tracking uses a discrete random walk (DRW) model for the turbulence dispersion (Chiu *et al.* 1999; Fluent 2012).

Kinetic model

The kinetics of the UV disinfection are widely assumed for a first-order chemical reaction with respect to the UV dose (Watson 1908). The typical UV response curve can be represented in two ways: a log survival curve and a log inactivation curve. Mathematically, the classical log-linear model form can be represented as follows:

$$\ln(N/N_0) = -KIt = -k[Dose] \quad (2)$$

where N_0 is pathogens influent, N is pathogens effluent, t is exposure time for UV, I is intensity of UV radiation, Dose is the dose of UV light, K is disinfection rate coefficient. Equation (2) represents the idealized conditions, based on the Chick–Watson law (Watson 1908).

Fluence rate model

The fluence rate field within the CCUV reactor was modelled using commercial software UVCalc3D, which is based on a multiple-segment source summation (MSSS)

fluence-rate modeling approach. There are two reasons for the use of UVCalc3D: (i) the facility of multiple band modeling and (ii) UVCalc3D's status as the only fluence rate model that is verified experimentally (Li *et al.* 2011). Therefore, the UV lamps employed in this research were MP lamps, and emission of the radiation from the UV lamps occurs in multiple peaks. Thus, the use of multiple banded modeling is imperative. In addition, the proposed GA methodology is equally applicable for a low pressure high output lamp.

The fluence modeling equation for the MSSS (UVCalc3D) model can be written as follows:

$$F' = \underbrace{\frac{P/N}{4\pi(d_1+d_2+d_3)^2}}_{\text{Point source}} \overbrace{(1-R_{12})(1-R_{23})}^{\text{Reflection at the medium}} \times \underbrace{T_w^{d_3/0.01} T_q^{d_2/0.01} Focus(\pi/4)\cos\theta_1}_{\text{attentuation within the medium}} \quad (3)$$

where P is the lamp power, N is the number of cylindrical segments, d_1 is the radial distance from a cylindrical segment to a lamp sleeve, d_2 is the air gap depth, d_3 is the distance of a point in the water medium, R_{12} is the reflectivity of the air–quartz interface, R_{23} is the reflectivity of the quartz–water interface, T_w is the water transmissivity, and T_q is the quartz sleeve transmissivity. The focus factor introduced by Liu *et al.* (2004) can be represented as follows:

$$\text{Focus} = (d_1+d_2+d_3)^2 \Delta\theta \cos\theta_1 / r(h_2-h_1)\cos\theta_3 \quad (4)$$

The focus factor accounts for the concentration of the UV light due to refraction; further details are given in the literature (Bolton 2000; Liu *et al.* 2004).

CFD ANALYSIS OF THE WATER-DISINFECTION UV REACTOR

Computational domain of the CCUV reactor

The geometry of the reactor is shown in Figure 2 taken from the literature (Chen *et al.* 2011). The diameter of the flow pipe was 0.320 m, and the direction of flow was along the x-axis. The orientation of the pipe was perpendicular to the axis of water flow. Four UV lamps were housed within a 0.039 mm-diameter quartz sleeve of the CCUV reactor. The computational domain (Figure 2) with an unstructured grid was 3 m long, including the entrance, exit, and the upstream and downstream pipes of the reactor.

Computational model description

The geometric modeling was done using CATIA V5R20, the meshing was done using ANSYS ICEM CFD, the CFD analysis was done using ANSYS FLUENT, and the optimization was accomplished using MATLAB. The input parameters were adopted as previously described by Munoz *et al.* (2007). The components for modeling the simulation are given in the flow chart in Figure 3.

The fluid in the reactor was water, and the effect of water heating by the lamps was neglected because the temperature increase was $<10\ ^{\circ}C$. Hence, there were no viscosity change effects. The SIMPLE algorithm was used for pressure–velocity coupling. The UV fluence field simulations were calculated using the UVCalc3D model, commercial software by Bolton Photosciences. The UV lamp was a 1 kW medium-pressure mercury lamp arranged and oriented transverse to the flow. There were four lamps in each case. Each lamp was housed within a cylindrical quartz sleeve having an electrical output efficiency of 30%

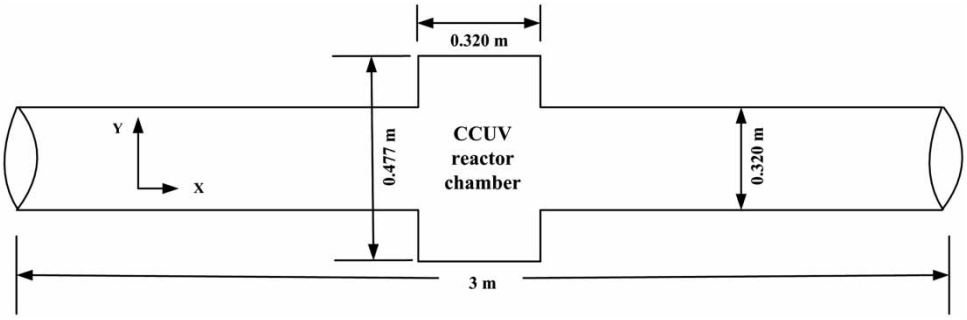

Figure 2 | Computational domain.

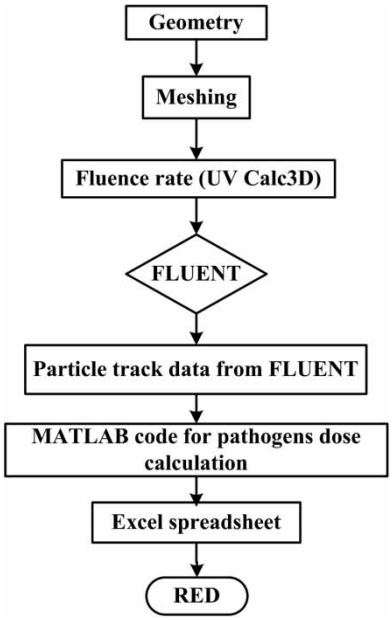

Figure 3 | Flow chart diagram of UV disinfection.

and an output spectrum equal to a typical MP lamp (Bolton 2000). The pathogens inactivation kinetics and the dose along each pathogen track were calculated using a user-defined function (UDF). The movement of the pathogens within the reactor was tracked using the Lagrangian particle tracking approach (Ducoste *et al.* 2005). The discretization of the convective term of the transport equation and the diffusion term were done using the second-order upwind scheme. The convergence criteria for the continuity, momentum, and turbulence equations for the normalized residuals were $<10^{-5}$ and for the fluence rate was $<10^{-6}$.

Boundary conditions

The boundary conditions for the CCUV reactor were defined as follows. A fluid velocity of 0.85 m/s was specified at the inlet. The RANS standard k-ε equations require the effects of turbulent kinetic energy k and turbulence dissipation ε. These parameters are compulsory for the inlet boundary conditions to define the standard k-ε turbulence model. Approximations of turbulent kinetic energy and turbulent dissipation were evaluated using Equations (5) and (6) (Liu *et al.* 2007).

$$k_{inlet} = (IU_{inlet})^2 \quad \text{where} \quad I = 0.05 \tag{5}$$

$$\varepsilon_{inlet} = k_{inlet}^{3/2}/0.01D \tag{6}$$

where U_{inlet} is the velocity at the inlet and D is the inlet pipe diameter of the CCUV reactor. The direction of the water flow was normal to the boundary. The computational domain was sufficient to ensure fully developed flow before entering into the chamber of the CCUV reactor. Furthermore, a UDF for the parabolic velocity profile was used at the inlet for fully developed flow. Pathogens were injected by defining an injection, and motion through the reactor was modelled using a Lagrangian approach. The injection defines the release conditions for the pathogens. This injection of pathogens was performed through file injection. The file was created using a FORTRAN code and providing injection parameters (pathogens diameter, mass flow rate, and number of pathogens to be injected). A fully developed flow (outflow) condition was ensured at the outlet. For the walls, a no-slip boundary condition and zero diffusive flux of the species were specified. The values for the multi-wavelength bands were based on the data provided by Bolton Photosciences Inc. (Bolton 2000).

Genetic-algorithm lamp-arrangement methodology

GAs are evolutionary algorithms that imitate the basic properties and fundamental mechanisms of natural evolution. GAs are distinct from conventional gradient-based optimization methods: (i) gradient information is not necessary; only the fitness value is involved; and (ii) GA does not progress sequentially from one point to the next; rather, many new points are calculated through iteration. The GA convergence is managed by the parameters, such as population size (Ps), probability of crossover (Pc), and probability of mutation (Pm).

Problem formulation

The lamp arrangement optimization problem can be defined as determining the position of the UV lamps within the chamber of the CCUV reactor such that the RED of the CCUV reactor is maximized. RED is a dose quantity used for providing an indication of the biological effects of the UV dose delivery by a UV disinfection system (USEPA 2006). A CCUV reactor having higher RED values is better than one having lower RED values.

The formulation of the lamp arrangement optimization problem is

$$\text{Maximization} \quad U = RED \tag{7}$$

$$\text{Subject to} \quad d = d_0 \qquad \varphi_{\min} \leq \phi_j \leq \phi_{\max}, \quad j = 1, 2, 3 \ldots .m \tag{8}$$

where U = objective function; d = lamp positioning diameter; d_0 = selected diameter for lamp arrangement; φ_j = angular position of each lamp; $\varphi_{\min}$, $\varphi_{\max}$ = minimum and maximum lamp arrangement angles; m = number of lamps.

The objective function of the optimization problem is the RED of the CCUV reactor calculated using Equations (7) and (8). The lamp arrangement optimization problem is solved using a GA, which is one of the most efficient optimization algorithms. The design variable are the positions of the UV lamps.

The GA consists of the following steps:

Step 1: Random population of the design variables is generated. This population consists of different parents and each parent is composed of different design variables. The design variables are the position of the UV lamps in the CCUV reactor.

Step 2: The CFD analysis is performed to calculate the fitness or objective function value. The objective function of the problem is the maximum RED value. This value is checked for fitness evaluation.

Step 3: By using the CFD results, fitness evaluation is achieved. Convergence is checked, and if the problem is converged, the process is stopped. If not, then it will go to the next step. The convergence criteria is solving the problem to the maximum defined number of iterations.

Step 4: Selection: the parents are selected by tournament selection to generate a new population. The objective function value of two parents are calculated and compared. The parent with a high objective function value is selected and other one is discarded.

Step 5: Single point crossover will produce the cut line in the two parents and join the first part of the first parent to the second part of the second parent, and vice versa, to generate two offspring. A cut line is created between the two parents to join the first part of the first parent to the second part of the second parent, and vice versa, to generate two more populations called children. This is called single point cross over.

Step 6: Mutation changes the one or more design variables in the child. The solution may change completely from the previous solution in the mutation. Therefore, a better solution can be achieved by using mutation. The mutation probability defines how often the parts of the population will be mutated. The mutation probability should be set low. If the mutation probability value is set too high, the search will turn into a random search.

Step 7: A new population has been produced by the above process.

Step 8: Go to step 2 with the new population, and repeat the process until the convergence criteria is satisfied.

The flow chart for the lamp arrangement optimization process using the GA is shown in Figure 4. The population of individuals is generated randomly. The fitness or objective function value of every individual in the population is evaluated. The fitness is the value of the objective function in the optimization problem. The fitness value is evaluated: if the fitness satisfies the convergence condition, the process is terminated; otherwise, it will continue for the next iteration. More individuals are selected from the current population and are mutated to form the new population. This new population is sent to evaluate the fitness by CFD analysis, and this fitness value is sent for assessment; this process continues until convergence is reached. The algorithm converges when the number of generations reaches the maximum number of iterations.

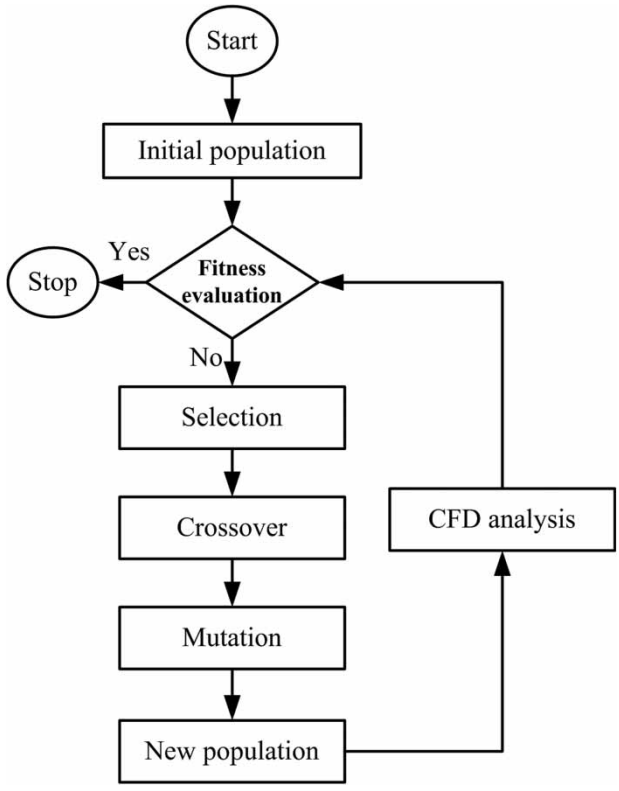

Figure 4 | Flow chart of lamp arrangement optimization.

RESULTS AND DISCUSSION

The impact of the lamp arrangement on the RED of the CCUV reactor was analyzed. The RED value is always determined by considering the target pathogen used, the ultraviolet transmittance (UVT), the flow rate, and the lamp status (USEPA 2006). The pathogens MS2 phage, 90% UVT (for 1 cm) of the water media, water flow velocity of 0.85 m/sec, and lamp power of 4 kW were kept constant for all the individuals. The best CCUV reactor is the one that achieves the highest RED value for a particular set of inputs. Therefore, keeping the input parameters constant provides a reasonable comparison basis among the reactors with the different lamp arrangements. All the lamps were identical, having lamp sleeve diameters of 39 mm and arc lengths of 477 mm, and the total electric power consumption was evenly shared among the CCUV reactors. The other dimensions of the CCUV reactor were kept constant, as shown in Figure 2.

Grid independence test

A comprehensive grid independence study was performed to ensure the grid independence of the results. There were two objectives of the grid independence test. First, the converged solution was obtained based on the boundary conditions and the physics involved, and not because of the mesh used. Second, the number of cells employed in the computational domain was optimized. The value of interest was the average velocity at the reactor outlet, and the optimum number of cells for the domain was >14 million, as illustrated in Figure 5.

Pathogen transport

The trajectories of pathogens were calculated by using a Lagrangian frame. The paths were calculated based on the particle force balance (drag force, gravitational force, and numerous other forces) integration. The pathogens were completely dispersed throughout the domain of the water. The pathogen–pathogen interactions were ignored, and the pathogens were considered to be spherical with their diameters provided. The velocity magnitude of the injected pathogen was not permitted to change after their collision with the boundary walls. The trajectory of each pathogen was calculated as it moved through the flow field.

For the fluent injection, a UDF was used to inject 3,000 particles at the inlet through file injection. The pathogens injection criteria to decide the number of particles for Lagrangian simulation were determined by Graham & Moyeed (2002) and achieved by Munoz *et al.* (2007) for the UV reactor. Considering similar criteria, we found that the number of pathogens required to

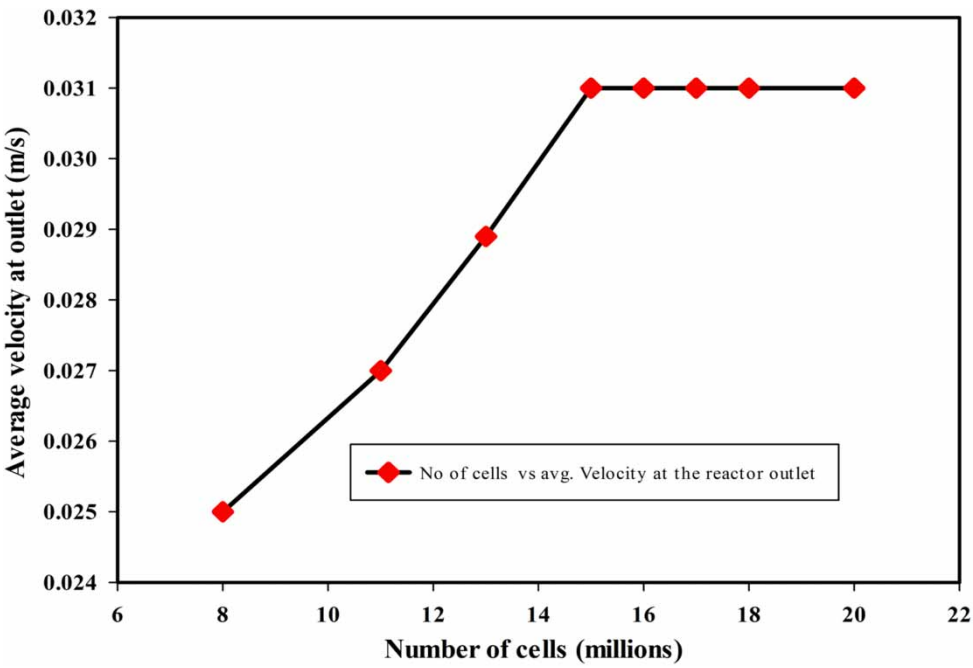

Figure 5 | Grid independence test.

obtain satisfactory results was >2,500. Therefore, 3,000 pathogens were injected through file injection at the inlet. The overall trajectory can be determined by using the DPM. Dispersion of particles due to turbulence in the flow was modelled by stochastic tracking using a DRW model (Chiu *et al.* 1999). The pathogen–pathogen interactions and the effects of the pathogen volume on the fluid were negligible.

The integral time scale is an important parameter of the DRW model, which defines the time consumed in the turbulent motion along the pathogen pathways. The value used for the integral time scale is the default value, as recommended in the literature (Munoz *et al.* 2007). The pathogen trajectories are shown in Figure 6, and the color coding used indicates the UV fluence rate. The trajectories of 100 pathogens are shown to provide good visualization. For the sake of better visualization, few pathogen tracks are shown in the bottom view of Figure 6.

Reduction equivalent dose

The UV dose can be described in two ways: average dose and RED. The concept of average dose cannot be employed for water disinfection because it can deviate from the final goal. Some of the treated pathogens can receive higher doses and others can receive lower doses.

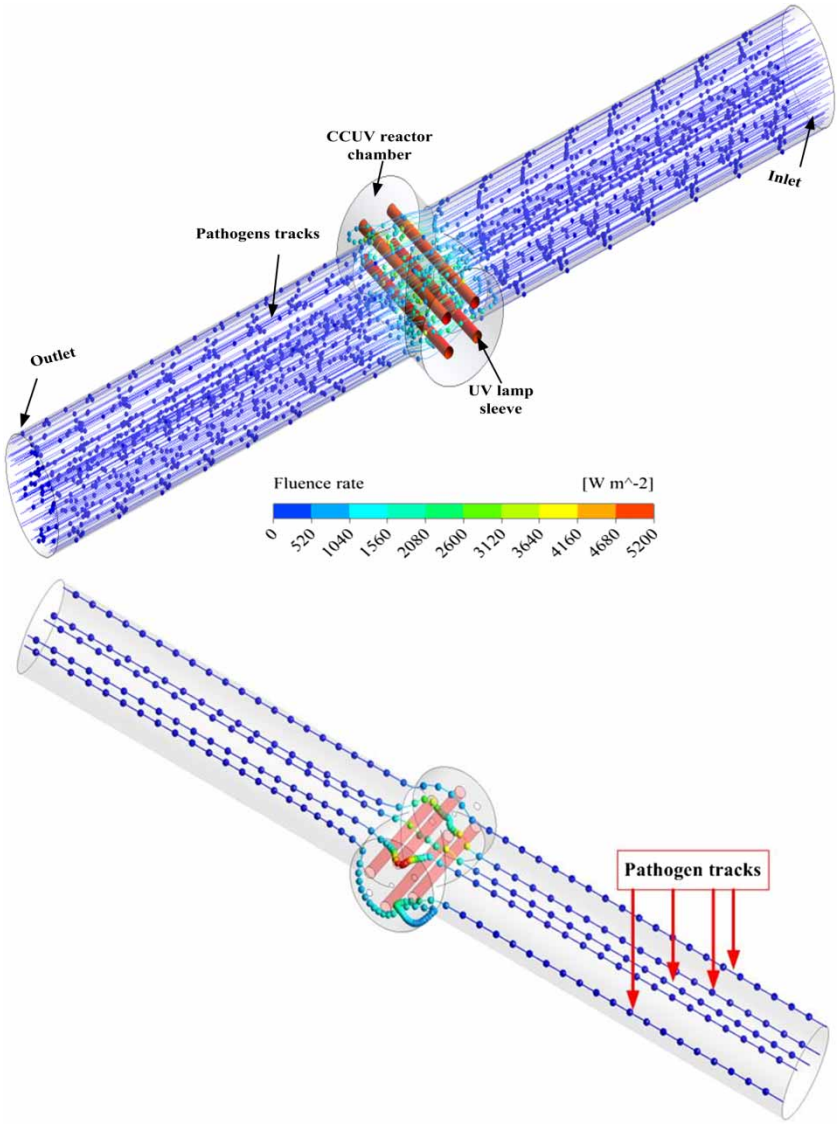

Figure 6 | Tracks of the pathogens colored according to fluence rate (number of tracks = 100). Please refer to the online version of this paper to see this figure in color: http://dx.doi.org/10.2166/wst.2016.119.

This can lead to erroneous results. Therefore, the concept of RED was employed. It predicts the minimum value of the dose that will be received by the pathogens. Hence, it ensures the targeted log reduction value throughout the water domain. RED is an indicator that shows the biological effects produced by the UV reactor. RED is usually measured using bio-dosimetry, a procedure that involves measurement of the inactivation of a challenge pathogen after exposure to UV light in the UV reactor and a comparison of the results to the known UV dose-response curve (USEPA 2006). RED value is always determined by considering factors like target pathogen used, UVT, flow rate, and lamp status. In this work, the UV dose was calculated in a semi-empirical way by using the following UV dose-response equation (USEPA 2006).

$$\mathrm{RED} = A\ \log\left(N_0/N\right) + B\ \log\left(N_0/N\right)^2 \tag{9}$$

where, $\log(N_0/N)$ = log inactivation; N_0 = pathogens influent; N = pathogens effluent.

A and B are the fitting coefficient for MS2 phage (USEPA 2006). The cumulative dose was calculated along each particle track, as shown in Figure 6, by using the in-house MATLAB code.

To analyze the effects of lamp arrangement on the performance of the water-disinfection CCUV reactor, both symmetric and asymmetric lamp arrangements within the chamber of CCUV reactor were considered.

OPTIMIZATION OF THE LAMP ARRANGEMENT

Symmetric lamp arrangement based on literature findings

Case study 1 — Effects of lamp arrangement diameter

The CCUV reactor used for the simulation is shown in Figure 2; it has a chamber diameter of 320 mm. To determine the optimum diameter for the lamp arrangement within the chamber of the reactor, the lamps were positioned at several diameters, as shown in Figure 7. These were developed by selecting a plane at the mid-span of the CCUV reactor. The fluence rate within the CCUV reactor was modeled by using UVCalc3D. The local intensity values were calculated under the assumption of 20-band MP mercury lamps with total output power of 4 kW over an arc length of 477 mm. The calculated fluence rate within the UV chamber varied abruptly, as shown in Figure 7. The fluence rate was high within the vicinity of the lamps and greatly decreased with increasing distance from the lamps.

To find the optimum diameter of the lamp arrangement circle, the lamps were positioned at diameters of 260, 230, 200, 170, 140, 110, and 90 mm within the chamber of the CCUV reactor. The deciding factor for the optimum diameter of the lamp arrangement was the maximum RED. Figure 8 provides further insight for the lamp arrangement circle. The graph shows that there is an optimum diameter for the lamp arrangement circle. Here, the optimum

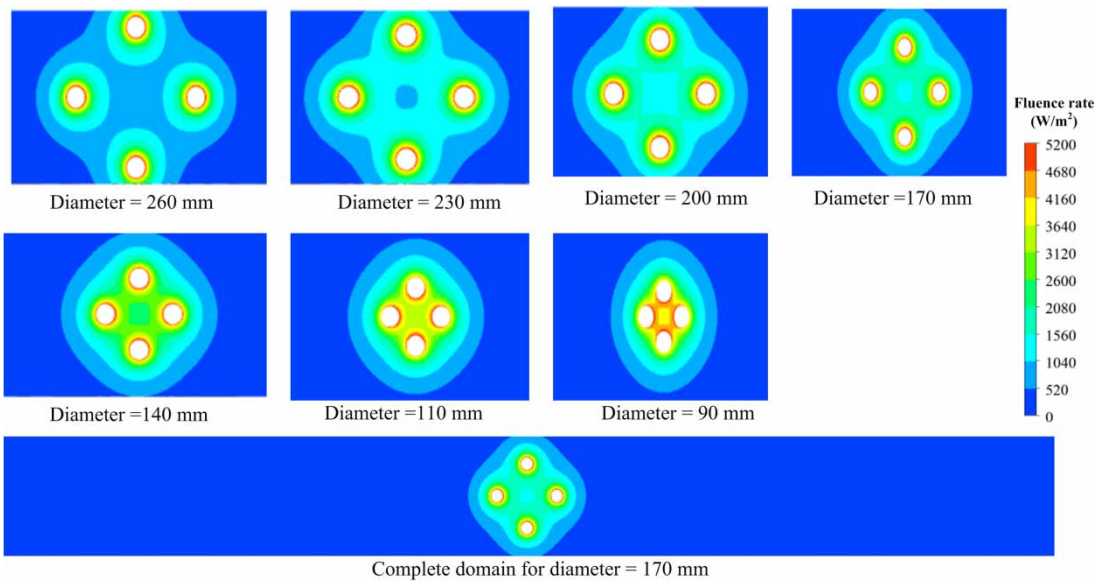

Figure 7 | UV fluence rate contours at different diameters.

diameter of the lamp arrangement circle was 170 mm. This will be called the optimum lamps circle from now on in this discussion. After analyzing Figure 8, we can predict that the optimum lamps circle lies within the following range:

$$\frac{D_c}{2} \pm 20 \text{ units} \tag{10}$$

where D_c is the diameter of the chamber of the CCUV reactor, which was 320 mm for the reactor under study. It was found that there is an optimum diameter of lamps circle, obtained using Equation (10), for optimized performance. This value should be determined for the optimized performance of the CCUV reactor. There was a 65% difference between the maximum and minimum RED values.

This percentage difference in RED values can be explained by the statement by Qualls & Johnson (1985) that closer proximity of the lamps to the walls and with each other results in a loss of UV dose. This percentage difference shows that determining the optimum diameter of the lamp arrangement is beneficial and should be part of CCUV reactor design and optimization.

Case study 2 – Effects of lamp arrangement angle

To analyze the effects of the lamp arrangement angle on the reactor performance, the angle was changed from 0 to 75 degrees in steps of 15 degrees. Figure 9 shows the UV fluence rate contours for different lamp arrangement angles.

As Figure 10 shows, there is an optimum lamp arrangement angle. It is 45 degrees for the CCUV reactor under study. Ray (1999) experimentally investigated a multiple hollow-tube reactor based on semiconductor photo catalysis, and described the existence of an optimal value for the incident angle of light that results in a radiation profile that is more evenly distributed and, thus, uniform catalyst activation. The current work focuses on the optimal value of the lamp arrangement angle that yields the highest RED value for the CCUV reactor.

To further investigate the reason that the optimum RED value is at 45 degrees, the average UV fluence rate (UV-AFR) received by the pathogens was evaluated at each angular position. These observations are plotted in Figure 11(a), which shows that the UV-AFR received by the pathogen is optimum at 45 degrees. Moreover, the average residence time (ART) of the pathogens was calculated, as shown in Figure 11(b). Although the effect of ART is very low, the effect of UV-AFR is significant because a higher value of received UV-AFR and a greater ART at 45 degrees result in the optimum RED value. Xu *et al.* (2015) stated that a good reactor should have high UV-AFR. Therefore, the lamp position angle of 45 degrees is best because it results in the highest UV-AFR. The lamp arrangement angle causes less than a 5% difference between the lowest and highest RED values. This analysis shows that an optimum lamp arrangement angle exists, and it should be considered for the design and optimization of the water-disinfection CCUV reactor.

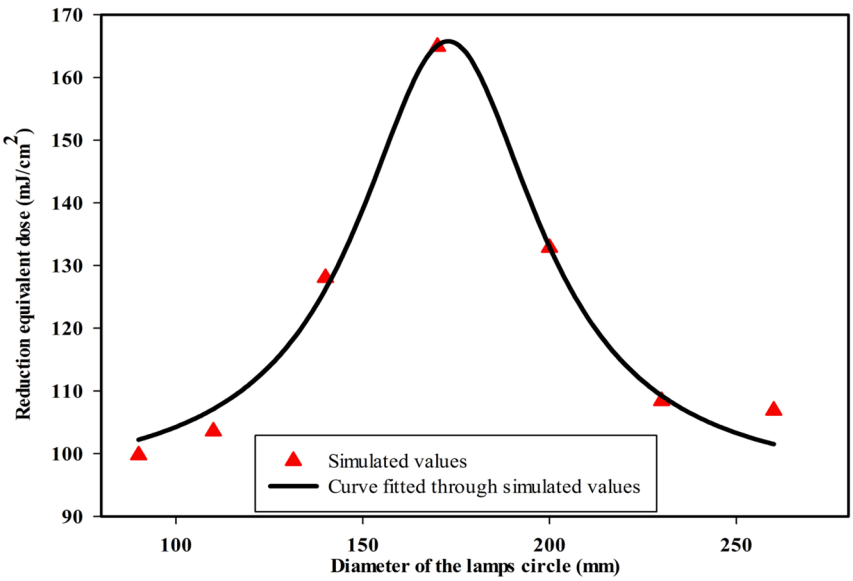

Figure 8 | Simulated RED values vs. lamp arrangements' diameter.

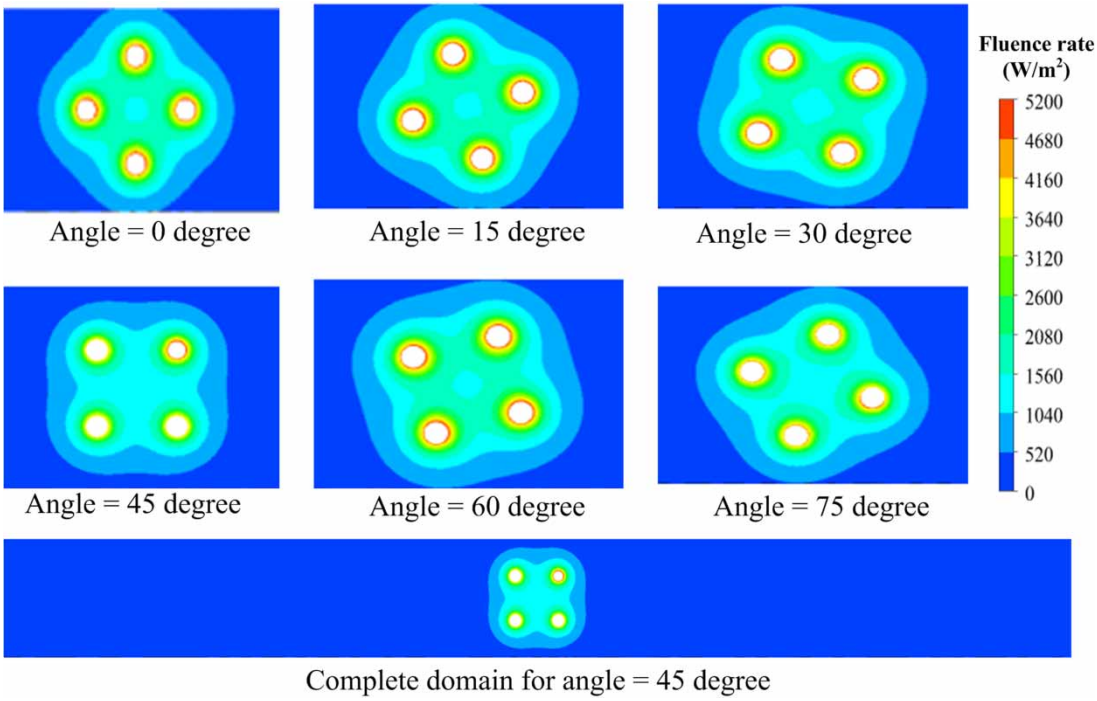

Figure 9 | UV fluence rate contours for different lamp arrangements' angles.

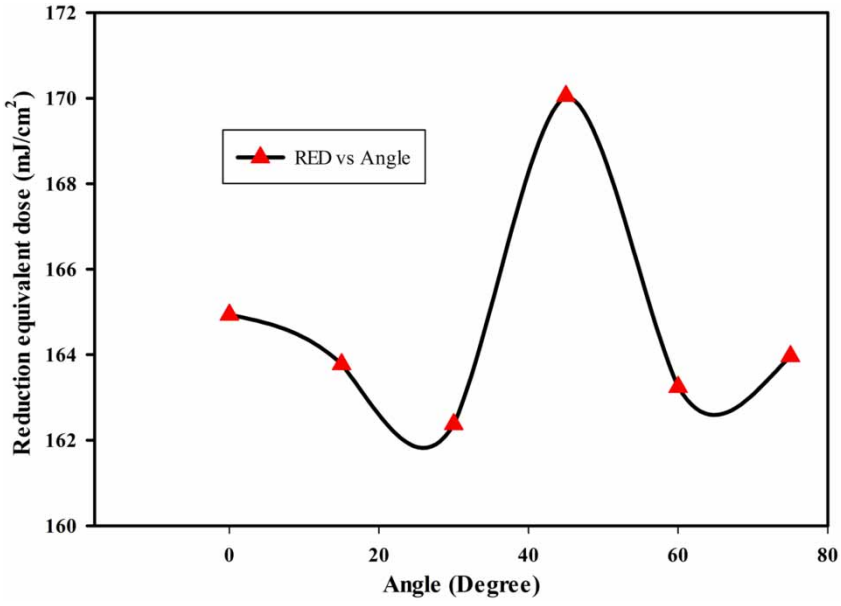

Figure 10 | Simulated RED values vs. angles of lamp arrangements.

Asymmetric lamp arrangement using genetic algorithm

As noted earlier, RED is greatly influenced by lamp arrangement and so cannot be ignored. To further investigate the effects of lamp arrangement, asymmetric lamp positions were also considered for analysis. Due to the large number of possible lamp arrangements, the problem was solved by using GA. We considered asymmetric lamp arrangement in two categories: (i) lying on the optimum lamps circle and (ii) lying on two circles within the optimum UV fluence zone.

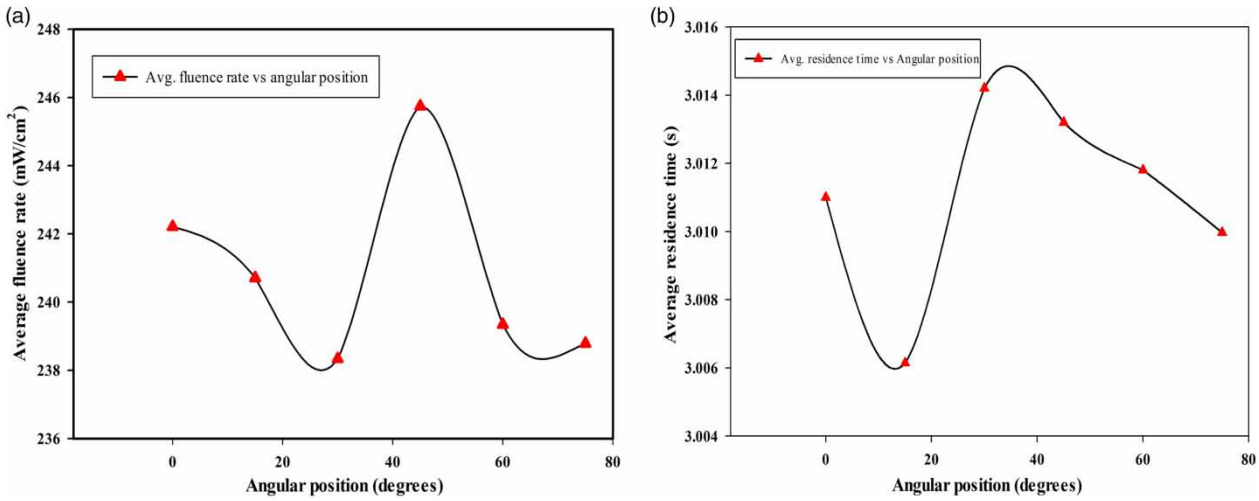

Figure 11 | Comparison of UV-AFR and ART vs. lamp arrangement angle.

Case study 3 – Effects of asymmetric lamp arrangement lying on the optimum lamps circle

Figure 8 shows the optimum lamps circle. To further investigate the effects of asymmetric lamp arrangement on the performance of the CCUV reactor, the position of the UV lamps were defined on the optimum lamps circle (170 mm) at 24 points. Each point was located at a difference of 15 degrees from the previous point, thus dividing the optimum lamps circle into 24 equiangular points, as shown in Figure 12. These 24 lamp positions are the design variables for the GA. One design variable was selected from each quadrant. There were four asymmetric lamp positions in each individual, which were determined using the GA-based lamp arrangement methodology, as shown in Figure 4. The total population generated was quite large. The total possible population is 1,290 for asymmetric case, but we set a maximum number of 20 iterations as convergence criteria. Figure 13 shows the UV fluence rate contour of the 20 individuals, which were determined using the GA-based lamp arrangement methodology.

The brief GA steps applied to this case study are as follows:

Step 1: The population was generated by selecting the one design variable from each quadrant. Few population are given below.

	Design variables			
Parent 1	1	8	14	21
Parent 2	1	7	13	23
Parent 3	2	10	15	22
Parent 4	2	11	17	20

Step 2: The objective function value of parents are calculated by using the CFD analysis.

	Design variables				Obj. function value
Parent 1	1	8	14	21	221.637
Parent 2	1	7	13	23	180.947
Parent 3	2	10	15	22	294.798
Parent 4	2	11	17	20	209.186

Step 3: The convergence criteria is set as solving the problem for a total of 20 iterations.

Step 4: The objective function value of the parents 1 and 2 and parents 3 and 4 are compared. The parent with the maximum objective function value in each pair is selected and others are discarded.

	Design variables				Obj. function value
Parent 1	1	8	14	21	221.637
Parent 3	2	10	15	22	294.798

Step 5: Each parent is cut in the middle and the first part of each parent is combined with the second part of other parent in order to produce child. This is called crossover. Two new populations have been generated in this way.

	Design variables				Obj. function value
Child 1	1	8	15	22	221.6375
Child 2	2	10	14	21	294.798

Step 6: Sometimes, anyone of the design variable in the population is replaced with any other design variable in mutation. But this mutation probability is

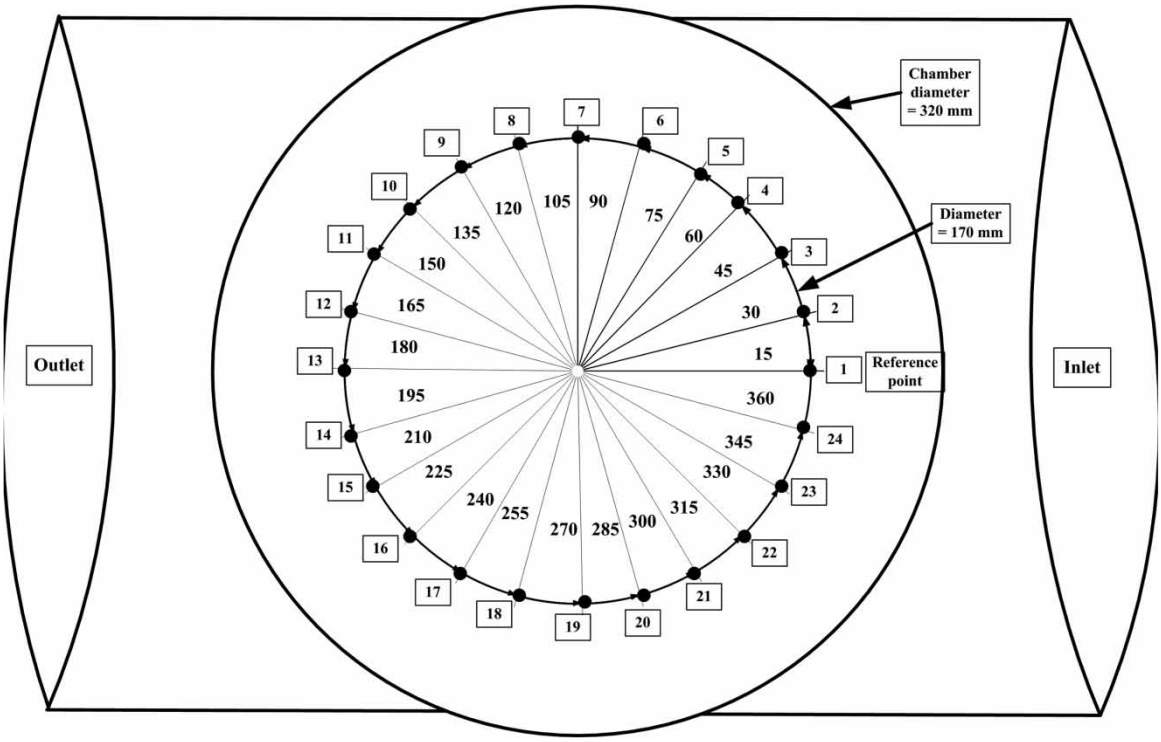

Figure 12 | Lamp arrangements on the optimum lamps circle.

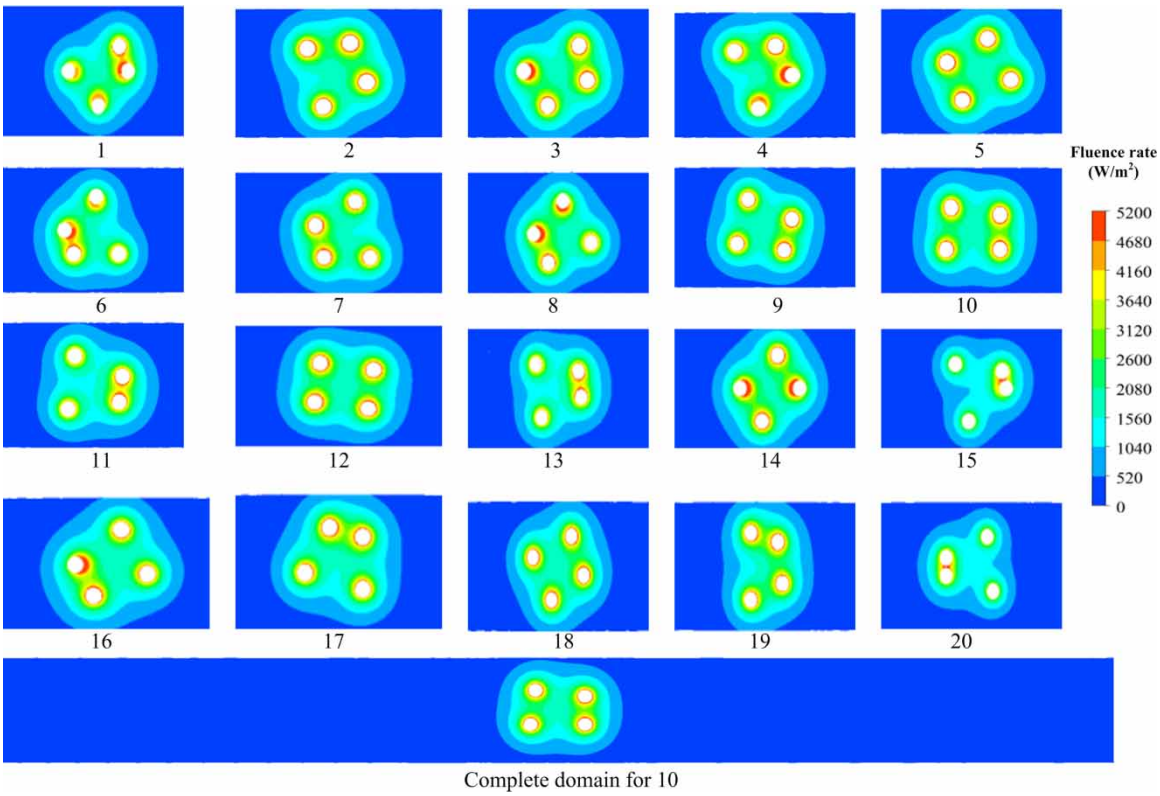

Figure 13 | UV fluence rate contours of asymmetric lamps positioned on the optimum lamps circle.

seldom selected in order to avoid the random search. We have changed the design variable 8 with 12 in child 1.

	Design variables			
Child 1	1	12	15	22
Child 2	2	10	14	21

Steps 7 and 8: A new population is created by the above steps and the process is repeated until the convergence is achieved.

Figure 14 shows that the asymmetric lamp arrangement significantly affects the CCUV reactor performance. This impact on performance, for both the angles and the diameters, is even greater with asymmetric than with symmetric lamp arrangement. Therefore, asymmetric lamp arrangements lying on the optimum lamps circle are better than symmetric ones, providing better UV dose delivery to the pathogens.

Figure 15 shows that lamp positions play an important role in the UV-AFR received and the ART of the pathogens. Again, the UV-AFR plays a noteworthy role in increasing RED values. Individuals having higher UV-AFR and more ART have higher RED values. As recommended by Xu *et al.* (2015), a better reactor is one that delivers higher UV-AFR to the pathogens.

Case study 4 – Effects of asymmetric lamp arrangement lying on two lamps circles

To further analyze the effects of lamp arrangement on the performance of the CCUV reactor, two lamp arrangement circles were chosen within the chamber of the CCUV reactor. The optimum lamps position is at the peak of the curve shown in Figure 8, so the two circles were positioned in that region.

The lamp arrangement circles had diameters of 160 and 180 mm, and the lamps had diameters of 39 mm, so the lamps were positioned within the peak region (the optimum UV zone). The lamp arrangement points were 30 degrees apart on the larger lamp arrangement circle (180 mm) and 45 degrees apart on the smaller lamp arrangement circle (160 mm), as shown in Figure 16. The positions of the lamps on the circle are the design variables for GA. The total possible population generated is 625 and 100 iterations are selected as convergence criteria. Each individual in the population consists of four design variables (four lamp positions) and one design variable is selected from each quadrant. Then, using the GA-based lamp arrangement methodology, shown in

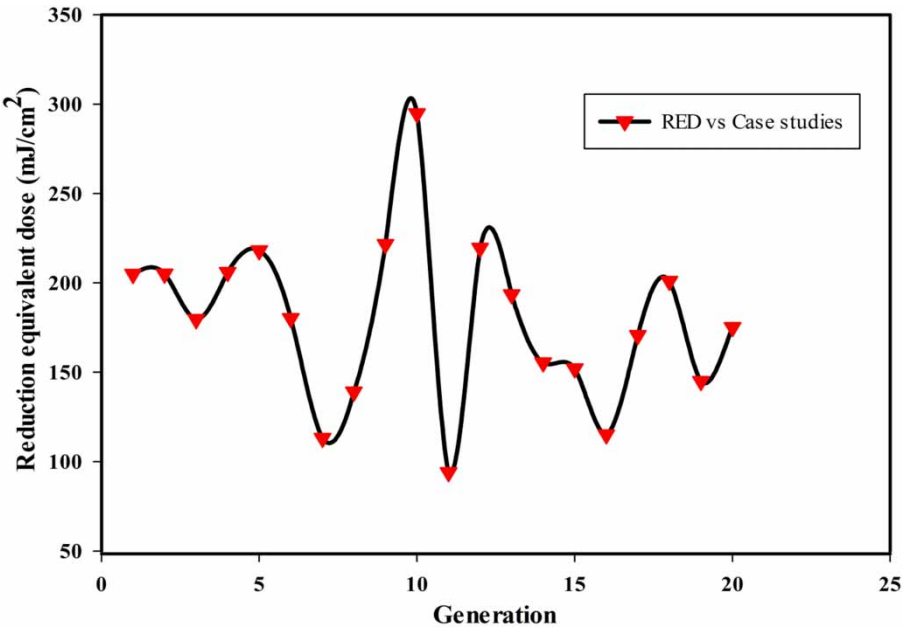

Figure 14 | Simulated RED values vs. generation in case study 3.

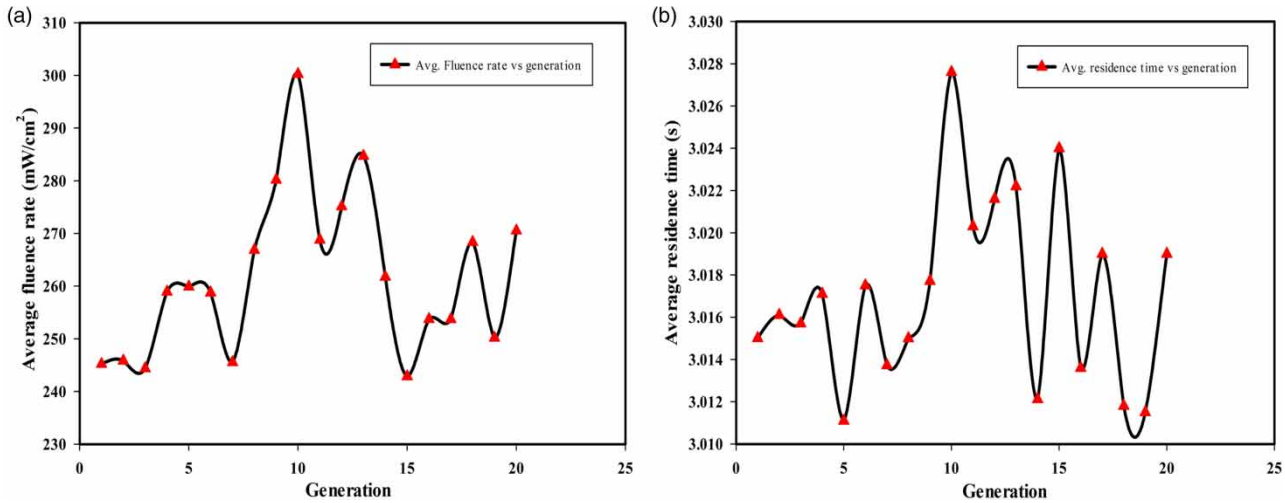

Figure 15 | Comparison of UV-AFR and ART vs. generation in case study 3.

Figure 4, the case study is solved. The brief GA steps are described here.

Step 1: Population generation: few populations are shown here.

	Design variables			
Parent 1	2	5	9	11
Parent 2	1	4	8	10
Parent 3	13	15	18	12
Parent 4	1	5	7	20

Step 2: Calculation of objective function value by using the CFD analysis.

	Design variables				Obj. function value
Parent 1	2	5	9	11	95.786
Parent 2	1	4	8	10	102.764
Parent 3	13	15	18	12	101.245
Parent 4	1	5	7	20	108.155

Step 3: Convergence criteria: 100 iterations for convergence.

Step 4: Selection: the comparison between objective function value of the pair of parents is made and the parent with higher objective function value is selected and others are discarded.

	Design variables				Obj. function value
Parent 2	1	4	8	10	102.764
Parent 4	1	5	7	20	108.155

Step 5: Crossover: the child is produced by crossover between parents.

	Design variables				Obj. function value
Child 1	1	4	7	20	105.315
Child 2	1	5	8	10	103.564

Step 6: Mutation is done to get the better solution.

	Design variables			
Child 1	1	4	7	20
Child 2'	1	5	18	10

Steps 7 and 8: The above steps produce new population and process is continued until convergence.

Figure 17 shows that the lamp arrangement on the two circles in the optimum performance zone, although the simulated RED of many individual results in very low values. The probable cause of the low RED value predicted for a number of individuals is the short circuiting (short UV exposure time and low UV fluence rate). A few individuals (17, 33, 41, and 98) have higher RED values. A rule of thumb for the lamp arrangement is that lamps should be neither closely packed together nor far apart, either of which results in a loss of UV dose.

Comparison of symmetric and asymmetric case studies

For a visual comparison of the case studies in this research work, the REDs of the symmetric and asymmetric cases are

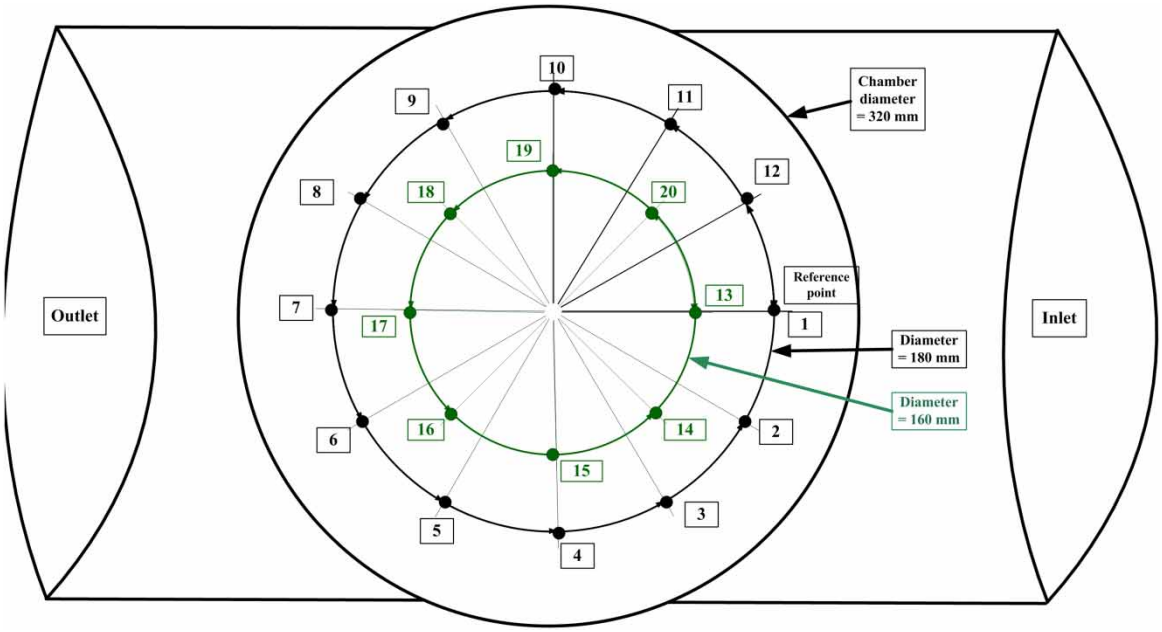

Figure 16 | Two lamp arrangements circles within the chamber of the CCUV reactor.

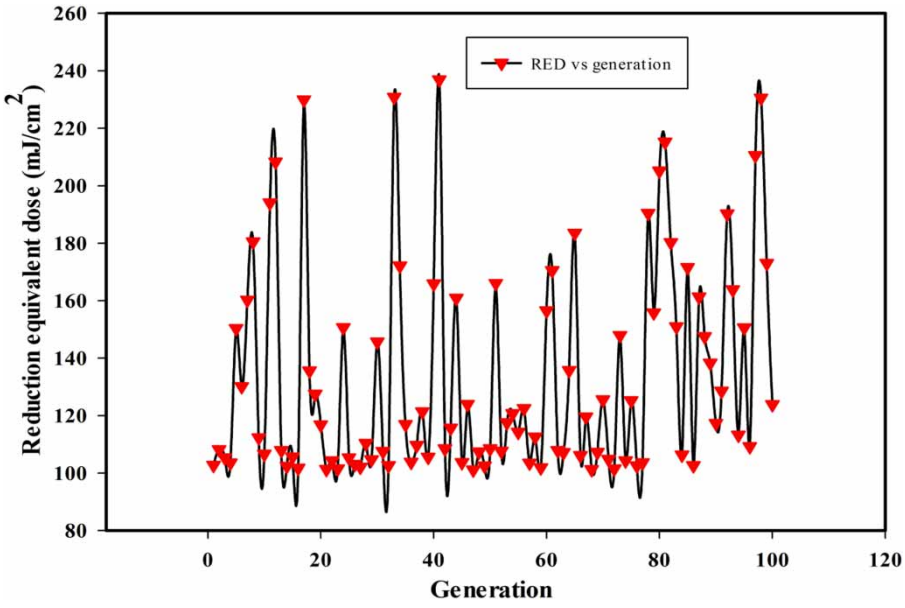

Figure 17 | Simulated RED values vs. generation in case study 4.

represented in the bar chart in Figure 18, including the minimum and maximum predicted RED values for each case study.

Figure 18 shows several significant outcomes of this research work. The case study scenarios significantly affect the performance optimization of the CCUV reactor. The minimum doses predicted for the case studies are almost the same, except for case study 2 for which case study 1 provided a starting point for further optimization. The highest RED value is predicted for case study 3, followed by case study 4, then case study 2, and finally case study 1 with the lowest RED value. The differences in evaluated RED values for these cases are explained in the discussion section.

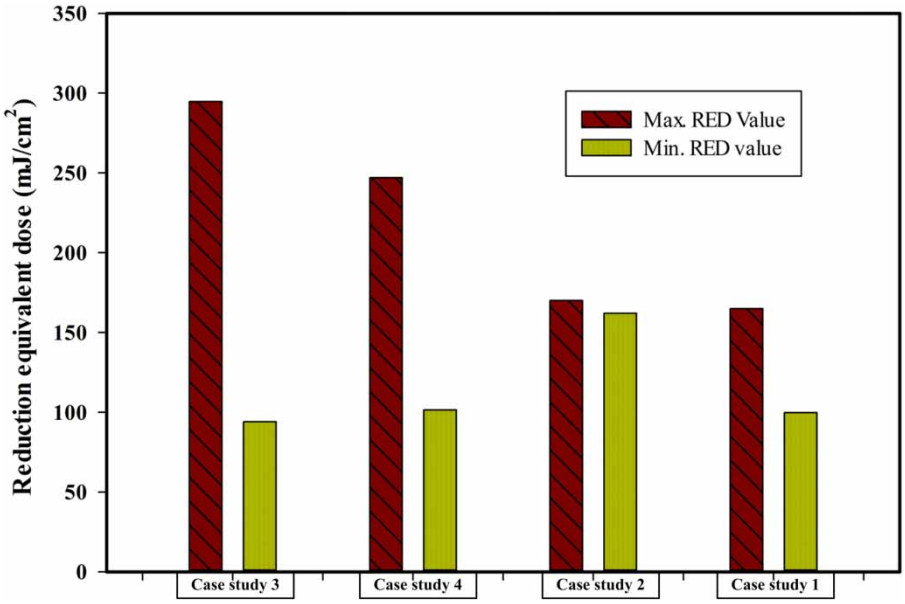

Figure 18 | Comparison of all the scenarios.

CONCLUSIONS

A lamp arrangement optimization method was proposed to optimize the performance of the water-disinfection CCUV reactor. This method is based on the UVCalc3D fluence rate model along with the standard k-ϵ turbulent model and kinetics, and it uses a GA-based methodology for lamp arrangement within the chamber of the CCUV reactor. The objective was to find the arrangement of lamps that maximizes the RED of the water-disinfection CCUV reactor. The following conclusions are drawn from this research work:

- There exists an optimum diameter of the lamps arrangement circle within the chamber of the CCUV reactor, which should be determined for the design and optimization of the CCUV reactor.
- The optimum lamps circle does not exist at the middle of the CCUV reactor chamber, but it should be searched for within the following range:

$$\left(\frac{D_c}{2} \pm 20 \text{ units}\right)$$

where D_c is the diameter of the CCUV reactor chamber.

- A judiciously placed symmetric lamp arrangement lying on the optimum lamps circle (with 170 mm diameter for the current CCUV reactor) optimizes the CCUV reactor performance.
- An asymmetric lamp arrangement on the optimum lamp circle yields better performance than a symmetric one because of higher UV-AFR.
- An asymmetric lamp arrangement on the two circles within the optimum UV zone results in better performance than a symmetric lamp arrangement. But an asymmetric lamp arrangement yields lower performance than the asymmetric lamp arrangement on the optimum lamp arrangement circle.
- The results show that the proposed GA-based lamp arrangement methodology for symmetric and asymmetric lamp arrangement can be used to obtain the optimum lamp arrangement.
- The proposed GA-based methodology for lamp arrangement was shown to be effective for the CCUV reactor, where, to date, there has been no well-defined mathematical relationship between the RED and the lamp arrangement.

The proposed lamp arrangement optimization methodology based on a GA shows promising results. Further, these findings are useful for extending the advanced oxidation production reactor studies along several dimensions for the investigation of optimized lamp arrangement criteria.

ACKNOWLEDGEMENTS

The authors would like to gratefully acknowledge NEOTEC UV, Seoul, Republic of Korea for providing the fluence

modeling tool UVCalc3D for this research work. Mr Tipu Sultan appreciates the financial support received from the Higher Education Commission (HEC), Pakistan, under the HRDI-UESTPs/UETs scholarship program.

REFERENCES

Bolton, J. R. 2000 Calculation of ultraviolet fluence rate distributions in an annular reactor: significance of refraction and reflection. *Water Res.* **34**, 3315–3324.

Chen, J., Deng, B. Q. & Kim, C. N. 2011 Computational fluid dynamics (CFD) modeling of UV disinfection in a closed-conduit reactor. *Chem. Eng. Sci.* **66**, 4983–4990.

Chiu, K., Lyn, D., Savoye, P. & Blatchley III, E. 1999 Integrated UV disinfection model based on particle tracking. *J. Environ. Eng.* **125**, 7–16.

Ducoste, J. J., Liu, D. & Linden, K. 2005 Alternative approaches to modeling fluence distribution and microbial inactivation in ultraviolet reactors: Lagrangian versus Eulerian. *J. Environ. Eng.* **131**, 1393–1403.

Fluent, A., 2012 14.5. Theory Guide 117.

Graham, D. I. & Moyeed, R. A. 2002 How many particles for my Lagrangian simulations? *Powder Technol.* **125**, 179–186.

Launder, B. E. & Spalding, D. 1974 The numerical computation of turbulent flows. *Comput. Method Appl. M.* **3**, 269–289.

Li, M., Qiang, Z., Li, T., Bolton, J. R. & Liu, C. 2011 In situ measurement of UV fluence rate distribution by use of a micro fluorescent silica detector. *Environ. Sci. Technol.* **45**, 3034–3039.

Liu, D., Ducoste, J., Jin, S. & Linden, K. 2004 Evaluation of alternative fluence rate distribution models. *Aqua* **53**, 391–408.

Liu, D., Wu, C., Linden, K. & Ducoste, J. 2007 Numerical simulation of UV disinfection reactors: evaluation of alternative turbulence models. *Appl. Math. Model* **31**, 1753–1769.

Munoz, A., Kresta, S. & Craik, S. A. 2007 Computational fluid dynamics for predicting performance of ultraviolet disinfection – sensitivity to particle tracking inputs. *J. Environ. Eng. Sci.* **6**, 285–301.

Qualls, R. G. & Johnson, J. D. 1985 Modeling and efficiency of ultraviolet disinfection systems. *Water Res.* **19**, 1039–1046.

Ray, A. K. 1999 Design, modelling and experimentation of a new large-scale photocatalytic reactor for water treatment. *Chem. Eng. Sci.* **54**, 3113–3125.

Renner, G. & Ekárt, A. 2003 Genetic algorithms in computer aided design. *Computer-Aided Design* **35**, 709–726.

Taghipour, F. 2004 Development of a CFD-based model for photo-reactor simulation. In: *Parallel Computational Fluid Dynamics 2003* (A. E. S. P. Fox, ed.). Elsevier, Amsterdam, The Netherlands, pp. 243–250.

Taghipour, F. & Sozzi, A. 2005 Modeling and design of ultraviolet reactors for disinfection by-product precursor removal. *Desalination* **176**, 71–80.

USEPA 2006 Ultraviolet Disinfection Guidance Manual for the Final Long Term 2 Enhanced Surface Water Treatment Rule Washington, DC.

Watson, H. E. 1908 A note on the variation of the rate of disinfection with change in the concentration of the disinfectant. *J. Hyg-Cambridge* **8**, 536–542.

Xu, C., Zhao, X. & Rangaiah, G. 2013 Performance analysis of ultraviolet water disinfection reactors using computational fluid dynamics simulation. *Chem. Eng. J. (Lausanne)* **221**, 398–406.

Xu, C., Rangaiah, G. & Zhao, X. 2014 Application of artificial neural network and genetic programming in modeling and optimization of ultra-violet water disinfection reactors. *Chem. Eng. Commun.* **292** (11), 1415–1424.

Xu, C., Rangaiah, G. P. & Zhao, X. S. 2015 A computational study of the effect of lamp arrangements on the performance of ultraviolet water disinfection reactors. *Chem. Eng. Sci.* **122**, 299–306.

First received 27 September 2015; accepted in revised form 16 February 2016. Available online 2 March 2016